Fast Diagrammatic Reasoning and Compositional Approaches to Fundamental Physics

Categorical semantics, causal structure and future directions

Topos Institute Colloquium

Jonathan Gorard

University of Cambridge
jg865@cam.ac.uk

April 29, 2021

Background of this Talk

Much of the recent work presented here was performed in collaboration with Manojna Namuduri and Xerxes Arsiwalla, e.g:

- J. Gorard, M. Namuduri, X. D. Arsiwalla (2021), `https://arxiv.org/abs/2103.15820`
- J. Gorard, M. Namuduri, X. D. Arsiwalla (2020), `https://arxiv.org/abs/2010.02752`
- J. Gorard (2021), `https://arxiv.org/abs/2102.09363`
- J. Gorard (2020), `https://arxiv.org/abs/2011.12174`

We will also present some forthcoming (and therefore necessarily more speculative) work towards the end, e.g:

- J. Gorard and X. D. Arsiwalla (WIP), *A Multiway Categorical Semantics for Petri Nets*
- J. Gorard and X. D. Arsiwalla (WIP), *A Diagrammatic Reasoning Language for Homotopy Type Theory*

Quantum Information from String Diagram Rewriting I

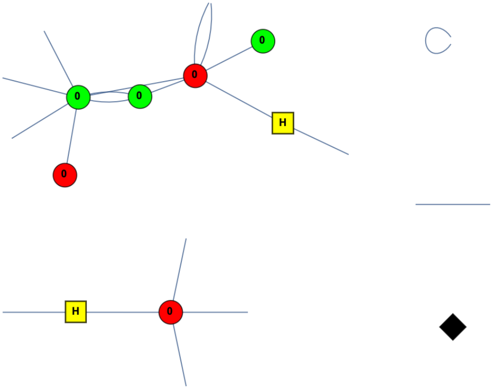

Figure: A linear transformation between finite-dimensional Hilbert spaces, represented as a ZX-diagram.

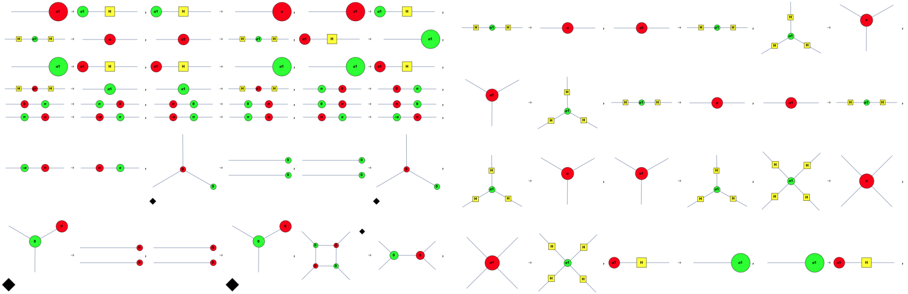

Figure: Samples of the complete rule enumeration for the ZX-calculus, as represented over all generators.

Quantum Information from String Diagram Rewriting III

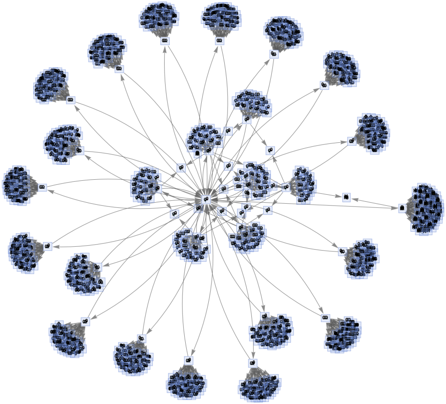

Figure: The multiway states graph corresponding to the first 2 steps in the non-deterministic evolution history of the ZX-calculus multiway operator system from a two-spider initial diagram.

General Relativity from Hypergraph Rewriting I

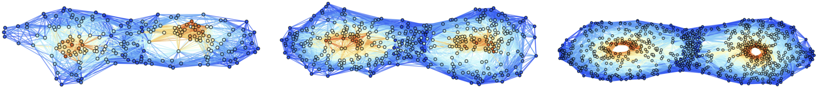

Figure: Spatial hypergraphs corresponding to the initial hypersurface configuration of the head-on collision of Schwarzschild black holes at time $t = 0M$, with resolutions of 200, 400 and 800 vertices, respectively, colored using the local curvature in the Schwarzschild conformal factor ψ.

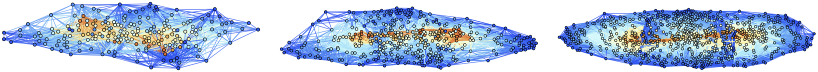

Figure: Spatial hypergraphs corresponding to the intermediate hypersurface configuration of the head-on collision of Schwarzschild black holes at time $t = 6M$, with resolutions of 200, 400 and 800 vertices, respectively, colored using the local curvature in the Schwarzschild conformal factor ψ.

General Relativity from Hypergraph Rewriting III

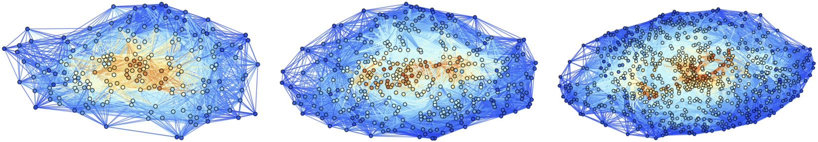

Figure: Spatial hypergraphs corresponding to the final hypersurface configuration of the head-on collision of Schwarzschild black holes at time $t = 12M$, with resolutions of 200, 400 and 800 vertices, respectively, colored using the local curvature in the Schwarzschild conformal factor ψ.

General Relativity from Hypergraph Rewriting IV

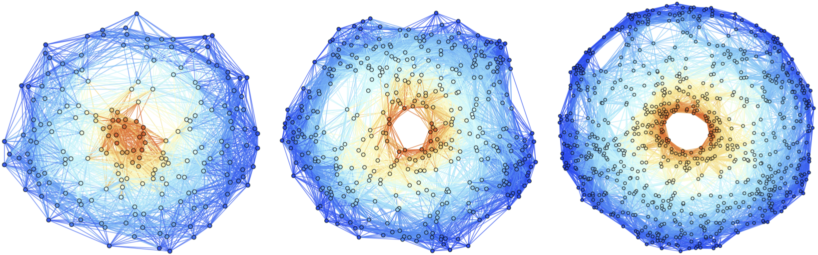

Figure: Spatial hypergraphs corresponding to the post-ringdown hypersurface configuration of the head-on collision of Schwarzschild black holes at time $t = 24M$, with resolutions of 200, 400 and 800 vertices, respectively, colored using the local curvature in the Schwarzschild conformal factor ψ.

General Relativity from Hypergraph Rewriting V

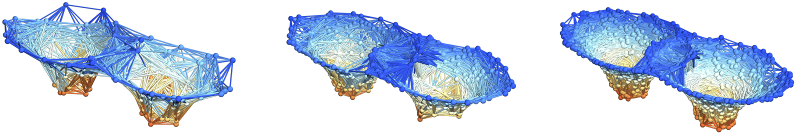

Figure: Spatial hypergraphs corresponding to projections along the z-axis of the initial hypersurface configuration of the head-on collision of Schwarzschild black holes at time $t = 0M$, with resolutions of 200, 400 and 800 vertices, respectively, colored and coordinatized using the local curvature in the Schwarzschild conformal factor ψ.

General Relativity from Hypergraph Rewriting VI

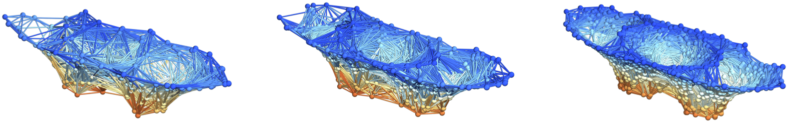

Figure: Spatial hypergraphs corresponding to projections along the z-axis of the intermediate hypersurface configuration of the head-on collision of Schwarzschild black holes at time $t = 6M$, with resolutions of 200, 400 and 800 vertices, respectively, colored and coordinatized using the local curvature in the Schwarzschild conformal factor ψ.

General Relativity from Hypergraph Rewriting VII

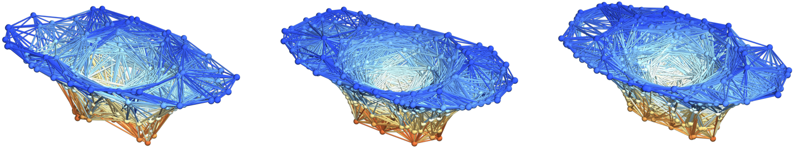

Figure: Spatial hypergraphs corresponding to projections along the z-axis of the final hypersurface configuration of the head-on collision of Schwarzschild black holes at time $t = 12M$, with resolutions of 200, 400 and 800 vertices, respectively, colored and coordinatized using the local curvature in the Schwarzschild conformal factor ψ.

General Relativity from Hypergraph Rewriting VIII

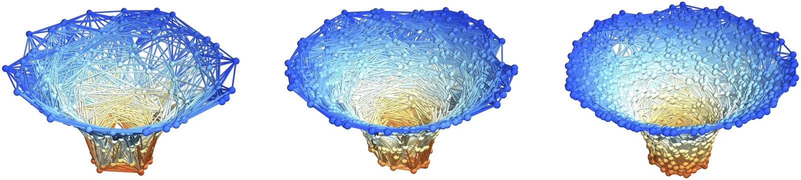

Figure: Spatial hypergraphs corresponding to projections along the z-axis of the post-ringdown hypersurface configuration of the head-on collision of Schwarzschild black holes at time $t = 24M$, with resolutions of 200, 400 and 800 vertices, respectively, colored and coordinatized using the local curvature in the Schwarzschild conformal factor ψ.

DPO Rewriting and the Wolfram Model I

We start with the category G:

$$\begin{tikzcd} E \arrow[r, bend left, "s"] \arrow[r, bend right, "t"'] & V, \end{tikzcd} \tag{1}$$

for objects E and V in $\mathrm{ob}(\mathsf{G})$, and morphisms s and t in $\hom(\mathsf{G})$.
Any given (multi-)graph G is a functor:

$$G : \mathsf{G} \rightarrow \mathsf{Set}, \tag{2}$$

with the category of directed (multi-)graphs Graph given by the functor category $[\mathsf{G}, \mathsf{Set}]$.
Can be extended to undirected (multi-)graphs or (multi-)hypergraphs by simply adding more morphisms to $\hom(\mathsf{G})$.

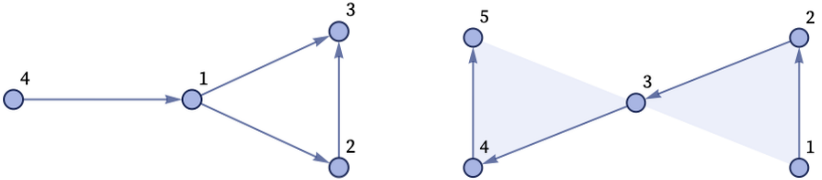

Figure: Two spatial hypergraphs, represented as finite collections of (un)ordered relations $\{\{1,2\},\{1,3\},\{2,3\},\{4,1\}\}$ and $\{\{1,2,3\},\{3,4,5\}\}$, respectively.

DPO Rewriting and the Wolfram Model III

Definition

A *rewrite rule* is a span of monomorphisms ρ:

$$\rho = (l : K \rightarrow L, r : K \rightarrow R). \tag{3}$$

Definition

A *rule match* is a morphism m:

$$m : L \rightarrow G. \tag{4}$$

DPO Rewriting and the Wolfram Model IV

Definition

A rewrite rule ρ is *applicable* at match m if there exists a pair of pushout diagrams:

$$\begin{tikzcd} L \arrow[d, "m"] & K \arrow[l, "l"'] \arrow[r, "r"] \arrow[d, "n"] & R \arrow[d, "p"] \\ G & D \arrow[l, "g"'] \arrow[r, "h"] & H \end{tikzcd} \tag{5}$$

We can extend these notions beyond the category Graph by considering arbitrary *adhesive* and *partial adhesive* categories.

DPO Rewriting and the Wolfram Model V

Definition

A *van-Kampen square* is a pushout $f' : B \to D$, $g' : C \to D$ in $\hom(\mathsf{C})$ of a span $g : A \to B$, $f : A \to C$ in $\hom(\mathsf{C})$, such that, for every commutative diagram:

$$\begin{tikzcd}
B' \arrow[dr, "h_B"] \arrow[ddd, "f'_h"'] & & & A' \arrow[lll, "g_h"'] \arrow[dl, "h_A"] \arrow[ddd, "f_h"] \\
& B \arrow[d, "f'"] & A \arrow[l, "g"'] \arrow[d, "f"] & \\
& D & C \arrow[l, "g'"'] & \\
D' \arrow[ur, "h_D"] & & & C' \arrow[lll, "g'_h"'] \arrow[ul, "h_C"']
\end{tikzcd} \tag{6}$$

such that pushouts and pullbacks are compatible.

DPO Rewriting and the Wolfram Model VI

Specifically, the van-Kampen square conditions applies whenever the subdiagrams:

$$\begin{tikzcd} B' & A' \arrow[l, "g_h"'] \arrow[d, "h_A"] \\ B & A \arrow[l, "g"] \end{tikzcd} \quad \text{with } B' \xrightarrow{h_B} B, \qquad \text{and} \qquad \begin{tikzcd} A \arrow[d, "f"] & A' \arrow[l, "h_A"'] \arrow[d, "f_h"] \\ C & C' \arrow[l, "h_C"] \end{tikzcd} \tag{7}$$

are both pullbacks.

Definition

An *adhesive category* is a category C that has pushouts along monomorphisms, that has pullbacks, and in which all pushouts along monomorphisms are van-Kampen squares.

Slice, coslice and functor categories always inherit adhesivity, but full subcategories do not in general.

DPO Rewriting and the Wolfram Model VII

Definition

A *partial adhesive category* is a full subcategory C' of an adhesive category C for which the embedding functor S:

$$S : \mathsf{C}' \to \mathsf{C}, \tag{8}$$

preserves monomorphisms.

Definition

An *S-span*, for a partial adhesive category C' with embedding functor $S : \mathsf{C}' \to \mathsf{C}$, is a diagram consisting of two maps f, g in $\hom(\mathsf{C}')$ sharing a common domain:

$$B \xleftarrow[f]{} A \xrightarrow{g} C, \tag{9}$$

for which a pushout diagram exists, and is preserved by S.

DPO Rewriting and the Wolfram Model VIII

Specifically, the diagram (an *S-pushout*):

$$\begin{array}{ccc} A & \xrightarrow{f} & B \\ \downarrow{\scriptstyle g} & & \downarrow{\scriptstyle p_1} \\ C & \xrightarrow{p_2} & P, \end{array} \tag{10}$$

should be preserved by the embedding functor.

Definition

An *S-pushout complement*, for a partial adhesive category C' with embedding functor $S : \mathsf{C}' \to \mathsf{C}$, for a pair of morphisms with overlapping domain and codomain $m : C \to A$, $g : A \to D$ in $\hom(\mathsf{C}')$, is a pair of morphisms with overlapping codomain and domain $f : C \to B$, $n : B \to D$ in $\hom(\mathsf{C}')$ such that a pushout diagram exists, and is an S-pushout.

DPO Rewriting and the Wolfram Model IX

Specifically, the following diagram should be an S-pushout:

$$
\begin{tikzcd}
C \arrow[r, "m"] \arrow[d, "f"] & A \arrow[d, "g"] \\
B \arrow[r, "n"] & D.
\end{tikzcd}
\tag{11}
$$

Definition

An *S-rule match*, for a partial adhesive category C' with embedding functor $S : \mathsf{C}' \rightarrow \mathsf{C}$, of a rewrite rule $\rho = (l : K \rightarrow L, r : K \rightarrow R)$, is a monomorphism $m : L \rightarrow G$ in $\hom(\mathsf{C}')$, for which the pair of morphisms with overlapping codomain and domain $l : K \rightarrow L$, $m : L \rightarrow G$ in $\hom(\mathsf{C}')$, have an S-pushout complement D for morphisms with overlapping codomain and domain $n : K \rightarrow D$, $g : D \rightarrow G$ in $\hom(\mathsf{C}')$.

DPO Rewriting and the Wolfram Model X

Specifically, the S-pushout complement has the general form:

$$\begin{tikzcd} K \arrow[r, "l"] \arrow[d, "n"] & L \arrow[d, "m"] \\ D \arrow[r, "g"] & G \end{tikzcd} . \tag{12}$$

Definition

A rewrite rule ρ is *S-applicable* at an S-rule match m, for a partial adhesive category C' with embedding functor $S : \mathsf{C}' \to \mathsf{C}$, if there exists a pair of S-pushout diagrams:

$$\begin{tikzcd} L \arrow[d, "m"] & K \arrow[l, "l"'] \arrow[r, "r"] \arrow[d, "n"] & R \arrow[d, "p"] \\ G & D \arrow[l, "g"] \arrow[r, "h"] & H \end{tikzcd} . \tag{13}$$

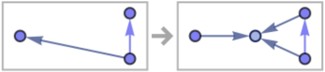

Figure: A hypergraph transformation rule, represented as a set substitution system $\{\{x, y\}, \{x, z\}\} \rightarrow \{\{x, y\}, \{x, w\}, \{y, w\}, \{z, w\}\}$.

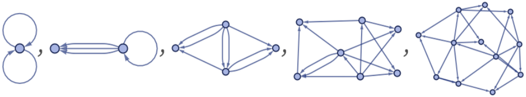

Figure: The hypergraphs obtained during the first four steps of evolution of the set substitution system $\{\{x, y\}, \{x, z\}\} \rightarrow \{\{x, y\}, \{x, w\}, \{y, w\}, \{z, w\}\}$, assuming an initial condition consisting of a single vertex with two self-loops.

DPO Rewriting and the Wolfram Model XII

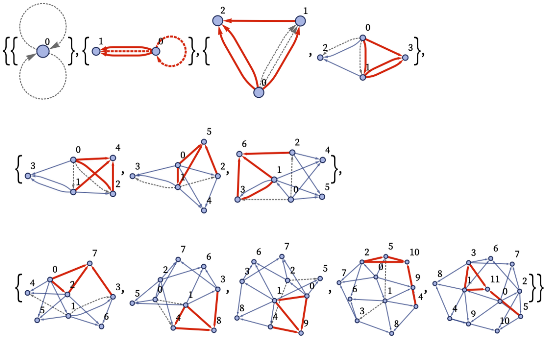

Figure: The non-overlapping (spacelike-separated) subhypergraphs involved in the rewrite events applied during the first four steps of evolution of the set substitution system $\{\{x, y\}, \{x, z\}\} \rightarrow \{\{x, y\}, \{x, w\}, \{y, w\}, \{z, w\}\}$, assuming an initial condition consisting of a single vertex with two self-loops.

Abstract Rewriting Structure and Multiway Systems I

If the rewrite relation $\rightarrow_R$ in the abstract rewriting system $(A, \rightarrow_R)$ is an indexed union of subrelations:

$$\rightarrow_R = \bigcup_i (\rightarrow_{i \in \Lambda}), \tag{14}$$

with index set Λ, then we obtained the labeled state transition system $(A, \Lambda, \rightarrow_R)$, i.e. a bijective map $\mathcal{P}(\Lambda \times A)$:

$$p \mapsto \{(\alpha, q) \in \Lambda \times A : p \mapsto_R^{\alpha} q\}. \tag{15}$$

Any such labeled state transition system is therefore described by an *F-coalgebra* for the power set functor $\mathcal{P}(\Lambda \times (-))$.

Abstract Rewriting Structure and Multiway Systems II

This correspondence holds because the power set construction on the category Set is a covariant endofunctor $\mathcal{P}$:

$$\mathcal{P} : \text{Set} \to \text{Set}. \tag{16}$$

Therefore, the abstract rewriting system $(A, \to_R)$ is simply an object A equipped with an additional morphism $\to_R$ of the category Set:

$$\to_R : A \to \mathcal{P}A. \tag{17}$$

Abstract Rewriting Structure and Multiway Systems III

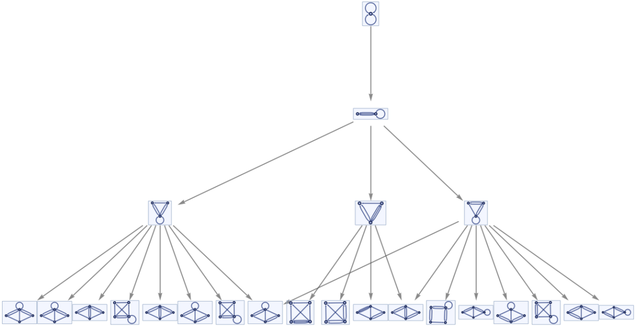

Figure: The first 3 steps in the non-deterministic evolution history for the set substitution rule $\{\{x, y\}, \{y, z\}\} \rightarrow \{\{w, y\}, \{y, z\}, \{z, w\}, \{x, w\}\}$, as represented by a multiway evolution graph.

Abstract Rewriting Structure and Multiway Systems IV

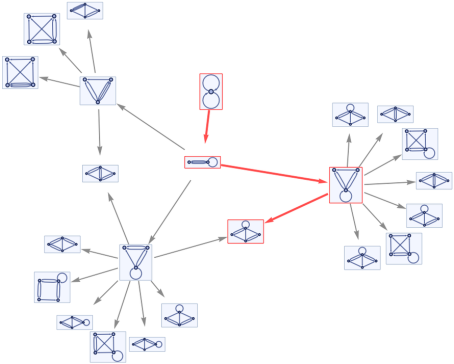

Figure: The first 3 steps in the *canonical* evolution history for the set substitution rule $\{\{x,y\},\{y,z\}\} \to \{\{w,y\},\{y,z\},\{z,w\},\{x,w\}\}$, as represented by a single path in the associated multiway evolution graph.

Multiway Systems as Monoidal Categories I

A multiway evolution graph is a category C equipped with a monoidal bifunctor $\otimes$:

$$\otimes : \mathsf{C} \times \mathsf{C} \to \mathsf{C}, \tag{18}$$

reflecting the fact that multiway evolution edges can be composed in parallel, as well as sequentially.

Since the multiway evolution edges can be inverted (by swapping L and R in the rule $\rho = (l : K \to L, r : K \to R)$), our category C is also a *dagger category*, since it comes equipped with a natural *involutive* functor $\dagger$:

$$\dagger : \mathsf{C}^{op} \to \mathsf{C}, \tag{19}$$

that is compatible with the monoidal structure $\otimes$.

Multiway Systems as Monoidal Categories II

Since every hypergraph $H = (V, E)$ possesses a corresponding dual $H^* = (V^*, E^*)$ (which is itself involutive, i.e. $(H^*)^* \cong H$), such that $V^* = \{e_i\}$, where $e_i \in E$, and $E^* = \{X_m\}$, where:

$$X_m = \{e_i | x_m \in e_i\}, \tag{20}$$

it follows that the dagger-symmetric monoidal category C is also *compact closed*.

Specifically, for every object A in $\mathrm{ob}(\mathsf{C})$, there exists a corresponding dual object A^* in $\mathrm{ob}(\mathsf{C})$ that is unique up to canonical isomorphism.

This *compact structure* designates an additional pair of morphisms η_A (the *unit*) and ϵ_A (the *counit*) in $\hom(\mathsf{C})$:

$$\eta_A : I \to A^* \otimes A, \qquad \text{and} \qquad \epsilon_A : A \otimes A^* \to I, \tag{21}$$

such that the monoidal structure $\otimes$, the dagger structure $\dagger$ and the compact structure (with unit η and counit ϵ) are all compatible.

Monoidal Example: ZX-Calculus I

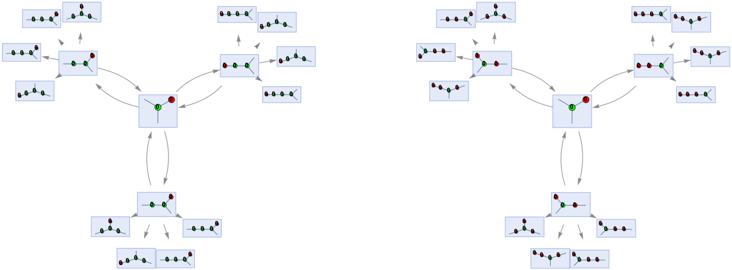

Figure: Multiway states graphs corresponding to the first 2 steps in the non-deterministic evolution history of the ZX-calculus multiway operator system, starting from a two-spider initial diagram, using only the (input arity 2 variants of the) Z- and X-spider identity rules, respectively.

Monoidal Example: ZX-Calculus II

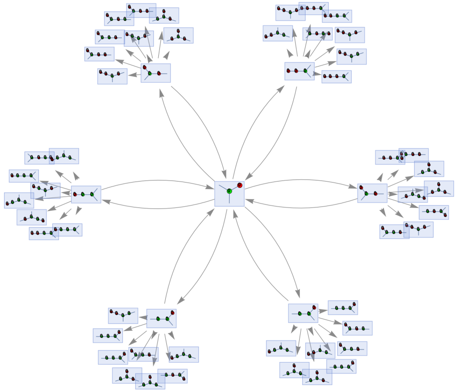

Figure: The multiway states graph corresponding to the first 2 steps in the non-deterministic evolution history of the composite ZX-calculus multiway operator system, starting from a two-spider initial diagram, using both the (input arity 2 variants of the) Z- and X-spider identity rules.

Monoidal Example: ZX-Calculus III

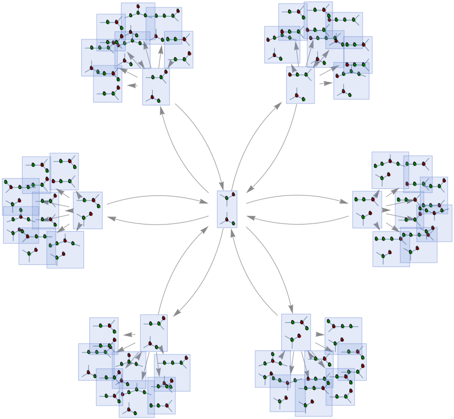

Figure: The multiway states graph corresponding to the first 2 steps in the non-determinsitic evolution history of the ZX-calculus multiway operator system, starting from a composite four-spider initial diagram, using only the (input arity 2 variant of the) Z-spider identity rule.

Monoidal Example: ZX-Calculus IV

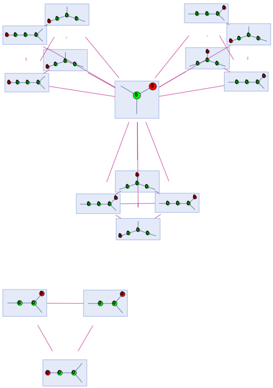 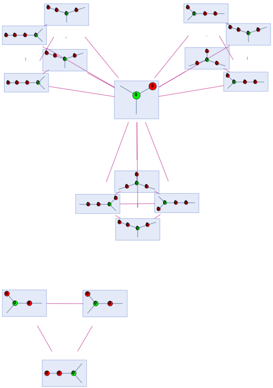

Figure: The corresponding branchial graphs, as witnessed within the default foliation of the multiway states graph for the ZX-calculus multiway operator system, starting from a two-spider initial diagram, using only the (input arity 2 variants of the) Z- and X-spider identity rules, respectively.

Monoidal Example: ZX Calculus V

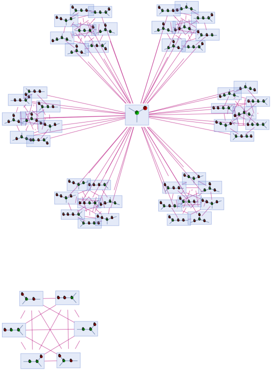

Figure: The corresponding branchial graph, as witnessed within the default foliation of the multiway states graph for the composite ZX-calculus multiway operator system, starting from a two-spider initial diagram, using both of the (input arity 2 variants of the) Z- and X-spider identity rules.

Monoidal Example: ZX-Calculus VI

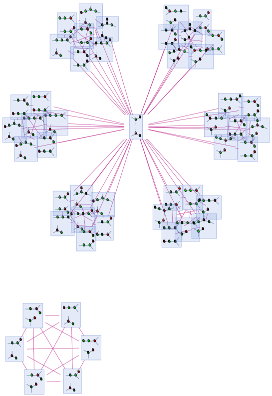

Figure: The corresponding branchial graph, as witnessed within the default foliation of the multiway states graph for the ZX-calculus multiway operator system, starting from a composite four-spider initial diagram, using only the (input arity 2 variant of the) Z-spider identity rule.

Causal Graphs as Partial Monoidal Categories I

Definition

A *causal graph*, denoted $G_{causal} = (V_{causal}, E_{causal})$, is a directed, acyclic graph associated to a given multiway evolution history, in which every vertex in V_{causal} corresponds to a rewrite, and in which the directed edge $a \to b$ exists in E_{causal} (for $a, b \in V_{causal}$) if and only if:

$$\mathrm{In}(b) \cap \mathrm{Out}(a) \neq \emptyset. \tag{22}$$

Thus, the transitive reduction of a causal graph yields the Hasse diagram for a causal partial order relation $\prec$ in the set of rewrites $\mathcal{C}$, such that:

$$\nexists x, y \in \mathcal{C}, \qquad \text{such that } x \prec y \text{ and } y \prec x, \tag{23}$$

and:

$$\forall x, y, z \in \mathcal{C}, \qquad x \prec y \text{ and } y \prec z \implies x \prec z. \tag{24}$$

Causal Graphs as Partial Monoidal Categories II

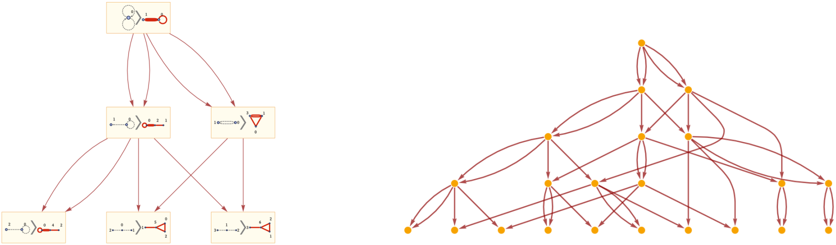

Figure: The causal graphs corresponding to the first 3 and 5 steps in the deterministic evolution history for the set substitution rule $\{\{x,y\},\{x,z\}\} \rightarrow \{\{x,y\},\{x,w\},\{y,w\},\{z,w\}\}$, respectively.

Causal Graphs as Partial Monoidal Categories III

Definition

A *partial functor* $F : \mathsf{B} \rightarrow \mathsf{C}$ between categories B (the *domain* of F) and C is a functor $\hat{F} : \mathsf{A} \rightarrow \mathsf{C}$, where A (the *domain of definition* of F) is a subcategory of B.

If the domain is a product category, then F is a *partial bifunctor*.
A causal graph is a category C equipped with a partial bifunctor $\otimes$ - the partial monoidal structure:

$$\otimes : \mathsf{C} \times \mathsf{C} \rightarrow \mathsf{C} \tag{25}$$

whose domain of definition $\mathrm{dd}(\otimes)$ is a full subcategory of its domain, along with a distinguished unit object I.

Necessary conditions (Coecke and Lal):

$$(A, I) \in \mathrm{dd}(\otimes), \qquad (I, A) \in \mathrm{dd}(\otimes), \qquad \text{and} \qquad A \otimes I = A = I \otimes A, \tag{26}$$

$$(A, B), (A \otimes B, C) \in \mathrm{dd}(\otimes) \qquad \iff \qquad (B, C), (A, B \otimes C) \in \mathrm{dd}(\otimes), \tag{27}$$

for any objects A, B and C in $\mathrm{ob}(\mathsf{C})$. Moreover, whenever objects $A \otimes (B \otimes C)$ and $(A \otimes B) \otimes C$ both exist, one has:

$$A \otimes (B \otimes C) = (A \otimes B) \otimes C. \tag{28}$$

Causal Graphs as Partial Monoidal Categories V

For any morphisms f, g and h in $\hom(\mathsf{C})$, whenever the morphisms $f \otimes (g \otimes h)$ and $(f \otimes g) \otimes h$ both exist, one has:

$$f \otimes (g \otimes h) = (f \otimes g) \otimes h. \tag{29}$$

Finally, whenever a pair of objects A and B exist in $\mathrm{ob}(\mathsf{C})$, such that:

$$(A, B), (B, A) \in \mathrm{dd}(\otimes), \tag{30}$$

there exists a symmetry morphism $\sigma_{A,B}$ of the form:

$$\sigma_{A,B} : A \otimes B \to B \otimes A, \tag{31}$$

with the property that:

$$\sigma_{A,B} \circ \sigma_{B,A} = id_{A \otimes B}. \tag{32}$$

Causal Graphs as Partial Monoidal Categories VI

In this way, our causal graphs are symmetric strict partial monoidal categories $(\mathsf{C}, \otimes, I)$ (symmetric strict because the α, λ and ρ isomorphisms are all identity isomorphisms).
We can think of these as being *causal categories* $(\mathsf{CC}, \otimes, I)$, for which every object A in $\mathrm{ob}(\mathsf{CC})$ has at least one element:

$$\mathsf{CC}(I, A) \neq \emptyset, \tag{33}$$

for which the unit object I in $\mathrm{ob}(\mathsf{CC})$ is terminal, i.e. for every object A in $\hom(\mathsf{CC})$, there exists a unique morphism $\top_A : A \to I$, and for which the monoidal product $A \otimes B$ (for objects A and B in $\mathrm{ob}(\mathsf{CC})$) exists if and only:

$$\mathsf{CC}(A, B) = [\mathsf{CC}(I, B)] \circ \top_A, \qquad \text{and} \qquad \mathsf{CC}(B, A) = [\mathsf{CC}(I, A)] \circ \top_B. \tag{34}$$

Multiway Evolution Causal Graphs

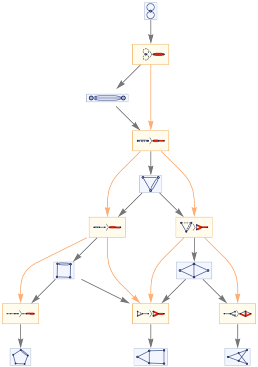

Figure: The multiway evolution causal graph corresponding to the first 4 steps in the non-deterministic evolution history for the set substitution rule $\{\{x, y\}, \{z, y\}\} \rightarrow \{\{x, w\}, \{y, w\}, \{z, w\}\}$ (with state vertices shown in blue, rewriting event vertices shown in yellow, evolution edges shown in gray and causal edges shown in orange.

A Categorical Semantics for Quantum Gravity?

Ultimately, out multiway evolution causal graphs appear to be (weak) 2-categories, with two different monoidal structures "knocking around": a dagger compact closed monoidal structure $\otimes_{\mathcal{M}}$ on the 1-morphisms (from the multiway evolution graph), and a symmetric strict partial monoidal structure $\otimes_{\mathcal{C}}$ on the 2-morphisms (from the causal graph).

Physical intuition: $\otimes_{\mathcal{M}}$ encodes the "quantum" aspects of the formalism, while $\otimes_{\mathcal{C}}$ encodes the "relativistic" aspects of the formalism, with the symmetry morphism $\sigma_{A,B}$ of $\otimes_{\mathcal{C}}$ encoding some kind of "spatial inversion" operation, etc.

Can potentially be formalized in terms of double categories, bicategories, ...?

The coherence and compatibility conditions between $\otimes_{\mathcal{M}}$ and $\otimes_{\mathcal{C}}$ effectively parametrize possible models for "quantum gravity".

Causal Semantics Example: ZX-Calculus I

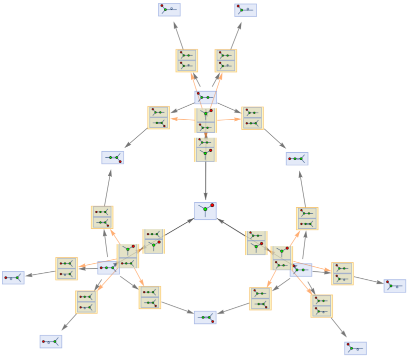

Figure: A subgraph of the multiway evolution causal graph corresponding to the first 2 steps in the non-deterministic evolution of the ZX-calculus multiway operator system, starting from a two-spider initial diagram (with state vertices shown in blue, rewriting event vertices shown in yellow, evolution edges shown in gray and causal edges shown in orange), restricted here to use only Z-spider identity rules.

Causal Semantics Example: ZX-Calculus II

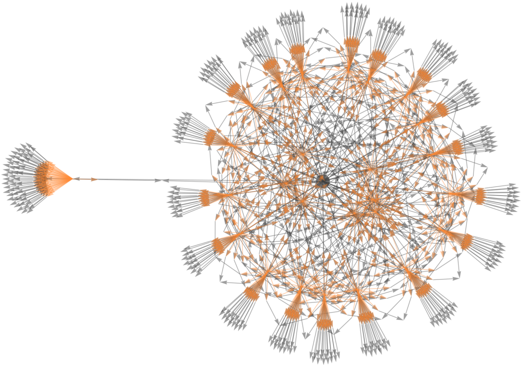

Figure: The multiway evolution causal graph corresponding to the first 2 steps in the non-deterministic evolution of the ZX-calculus multiway operator system, starting from a two-spider initial diagram (with state vertices shown in blue, rewriting event vertices shown in yellow, evolution edges shown in gray and causal edges shown in orange), with no restrictions.

Equational Reasoning with Causal Structure I

By ordering equational terms using a selection function S based on their causal edge density, we construct a refutation-complete proof calculus for first-order diagrammatic logic (with equality) that generalizes the standard Knuth-Bendix unfailing completion procedure.

Specifically, we introduce the inference rules of *selective resolution*:

$$\frac{\Lambda \cup \{u \approx v\} \implies \Pi}{\Lambda\sigma \implies \Pi\sigma}, \tag{35}$$

selective superposition:

$$\frac{\Gamma \implies \Delta \cup \{s \approx t\} \qquad \{u[s'] \approx v\} \cup \Lambda \implies \Pi}{\{u[t]\sigma \approx v\sigma\} \cup \Gamma\sigma \cup \Lambda\sigma \implies \Delta\sigma \cup \Pi\sigma}, \tag{36}$$

and ordered resolution:

$$\frac{\Gamma \implies \Delta \cup \{P(s_1, \dots, s_n) \approx tt\} \qquad \{P(t_1, \dots, t_n) \approx tt\} \cup \Lambda \implies \Pi}{\Gamma\sigma \cup \Lambda\sigma \implies \Delta\sigma \cup \Pi\sigma}.$$

Equational Reasoning with Causal Structure II

Within these inference rules, $u \approx v$ is any occurrence of an equation within the clause:

$$\{u \approx v\} \cup \Lambda \implies \Pi, \tag{38}$$

that is maximal with respect to the selection function S.
A tedious and elaborate construction allows us to define a morphism Θ between higher-order diagrammatic logics $\mathcal{L}^n$ and first-order multisorted logic $\mathcal{L}^1_{sort}$ (with equality):

$$\Theta : \mathcal{L}^n(\mathcal{S}) \to \mathcal{L}^1_{sort}(\Theta(\mathcal{S})), \tag{39}$$

mapping sets of formulas $\mathcal{F}$ in the higher-order logic $\mathcal{L}^n(\mathcal{S})$ to sets of formulas in the first-order multisorted logic $\mathcal{L}^1_{sort}(\Theta(\mathcal{S}))$:

$$\Theta : \mathcal{F}(\mathcal{L}^n(\mathcal{S})) \to \mathcal{F}(\mathcal{L}^n_{sort}(\Theta(\mathcal{S}))). \tag{40}$$

Theorem-Proving over Wolfram Model Systems I

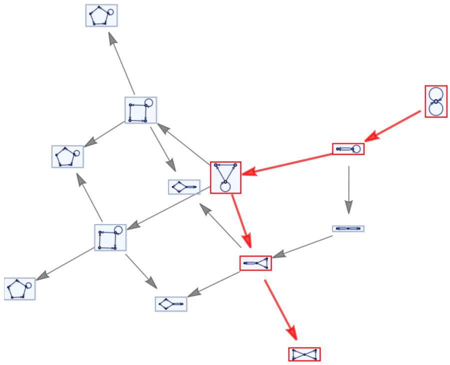

Figure: The first 4 steps in the non-deterministic evolution history for the set substitution rule $\{\{x, y\}, \{x, z\}\} \to \{\{x, z\}, \{x, w\}, \{y, w\}\}$, as represented by a multiway evolution graph, with the path between states $\{\{0, 0\}, \{0, 0\}\}$ and $\{\{0, 1\}, \{0, 3\}, \{1, 3\}, \{0, 2\}, \{0, 4\}, \{2, 4\}\}$ highlighted.

Theorem-Proving over Wolfram Model Systems II

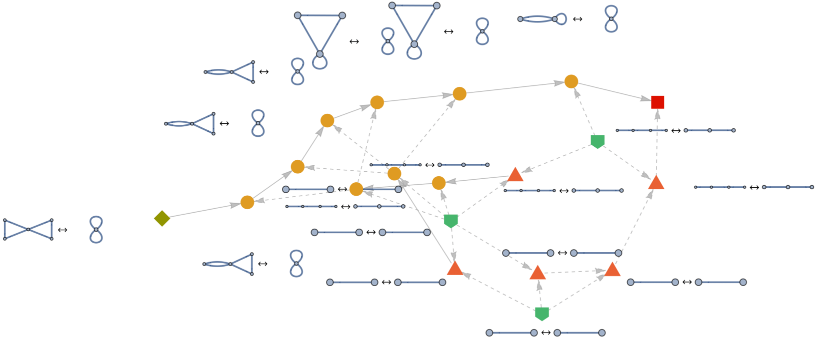

Figure: The proof graph corresponding to the proof of the proposition that state $\{\{0,1\},\{0,3\},\{1,3\},\{0,2\},\{0,2\},\{0,4\},\{2,4\}\}$ is reachable from initial state $\{\{0,0\},\{0,0\}\}$, subject to the set substitution rule $\{\{x,y\},\{x,z\}\} \rightarrow \{\{x,z\},\{x,w\},\{y,w\}\}$.

Theorem-Proving over Wolfram Model Systems III

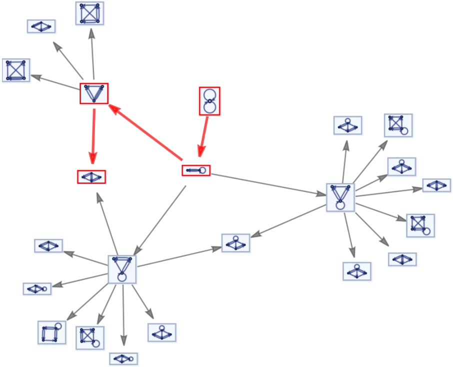

Figure: The first 3 steps in the non-deterministic evolution history for the set substitution rule $\{\{x, y\}, \{x, z\}\} \rightarrow \{\{x, z\}, \{x, w\}, \{y, w\}, \{z, w\}\}$, as represented by a multiway evolution graph, with the path between states $\{\{0, 0\}, \{0, 0\}\}$ and $\{\{0, 1\}, \{0, 2\}, \{0, 2\}, \{1, 2\}, \{0, 1\}, \{0, 3\}, \{1, 3\}, \{1, 3\}\}$ highlighted.

Theorem-Proving over Wolfram Model Systems IV

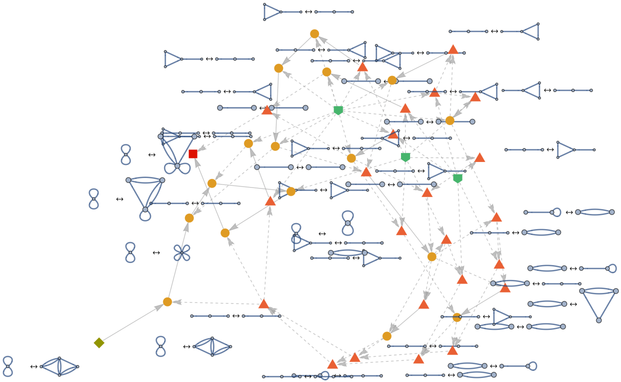

Figure: The proof graph corresponding to the proof of the proposition that state $\{\{0,1\},\{0,2\},\{0,2\},\{1,2\},\{0,1\},\{0,3\},\{1,3\},\{1,3\}\}$ is reachable from initial state $\{\{0,0\},\{0,0\}\}$, subject to the set substitution rule $\{\{x,y\},\{x,z\}\} \to \{\{x,z\},\{x,w\},\{y,w\},\{z,w\}\}$.

Theorem-Proving in the ZX-Calculus I

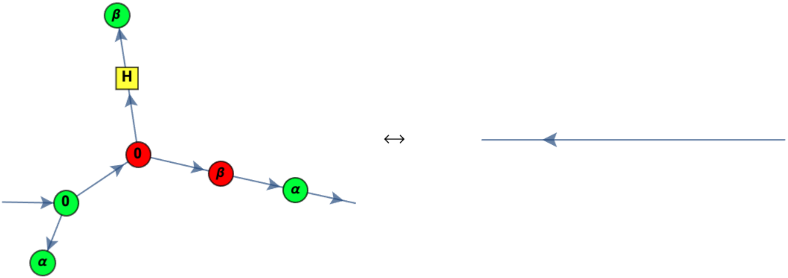

Figure: The statement of correctness for a complete quantum teleportation protocol, represented as a theorem in the ZX-calculus.

Theorem-Proving in the ZX-Calculus II

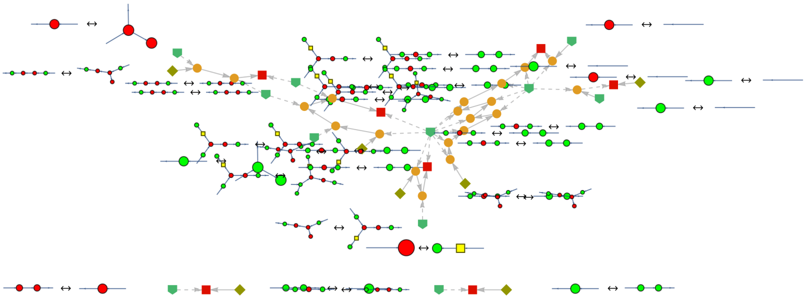

Figure: The proof graph corresponding to the proof of correctness for the complete quantum teleportation protocol, subject to the rules of the ZX-calculus.

Performance Test (Quantum Circuit Simplification) I

We test the algorithm against two common classes of circuit simplification task in quantum information theory: the diagrammatic reduction of Clifford circuits to a pseudo-normal form (graph state with local Cliffords), and the diagrammatic simplification of non-Clifford circuits via reduction of T-count.

These tests are performed using randomly-generated quantum circuits up to 3000 gates in size, both with and without causal optimization, and comparing both time complexity and proof complexity.

The method is found to comparable very favorably against pre-existing software frameworks and algorithms, such as *PyZX* and *Quantomatic*.

Performance Test (Quantum Circuit Simplification) II

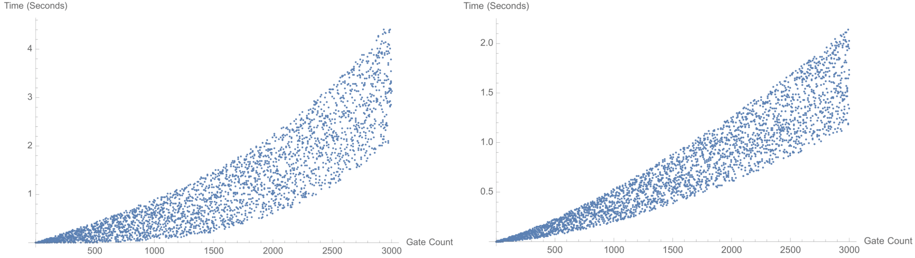

Figure: Plots showing the time complexity (in seconds) of the automated theorem-proving algorithm when reducing randomly-generated Clifford circuits with sizes up to 3000 gates down to pseudo-normal form, both with (right) and without (left) causal optimization.

Performance Test (Quantum Circuit Simplification) III

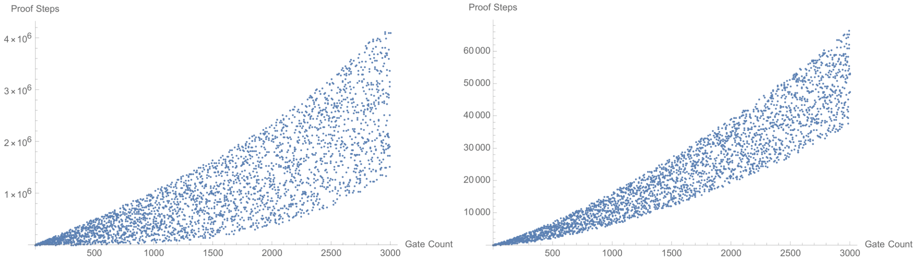

Figure: Plots showing the proof complexity (in proof steps) of the proofs generated by the automated theorem-proving algorithm when reducing randomly-generated Clifford circuits with sizes up to 3000 gates down to pseudo-normal form, both with (right) and without (left) causal optimization.

Performance Test (Quantum Circuit Simplification) IV

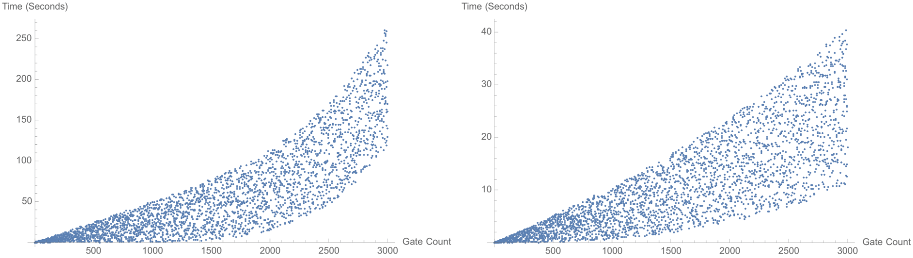

Figure: Plots showing the time complexity (in seconds) of the automated theorem-proving algorithm when minimizing the number of T-gates in randomly-generated non-Clifford circuits, both with (right) and without (left) causal optimization.

Performance Test (Quantum Circuit Simplification) V

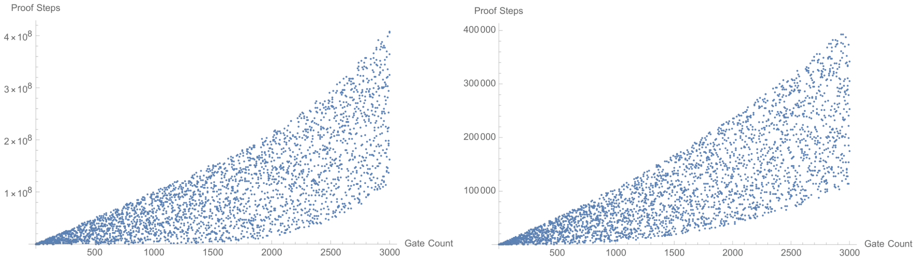

Figure: Plots showing the proof complexity (in proof steps) of the proofs generated by the automated theorem-proving algorithm when minimizing the number of T-gates in randomly-generated non-Clifford circuits, both with (right) and without (left) causal optimization.

Future Work: Petri Nets I

Dealing now with the adhesive HLR category PTNets...

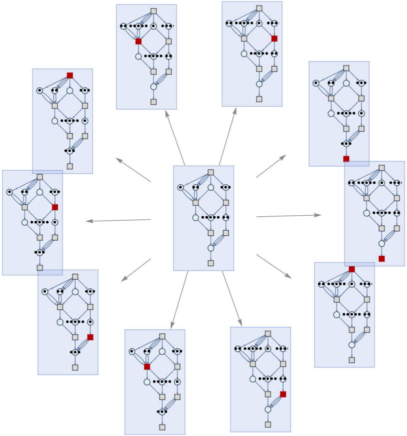

Figure: Multiway states graph corresponding to the first step in the non-deterministic evolution history of a Petri net multiway system.

Future Work: Petri Nets II

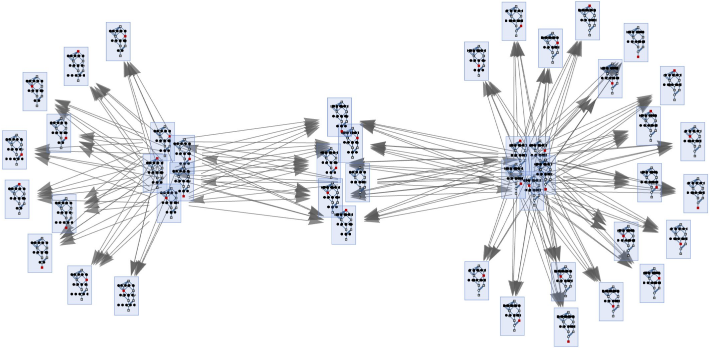

Figure: Multiway states graph corresponding to the first 2 steps in the non-deterministic evolution history of a Petri net multiway system.

(SPO works like a Petri net with read and reset arcs. DPO works like Petri nets with read and inhibitor arcs.)

Future Work: HoTT I

Proof graphs themselves are diagrammatic structures (i.e. labeled digraphs). Can we define a corresponding reasoning language?

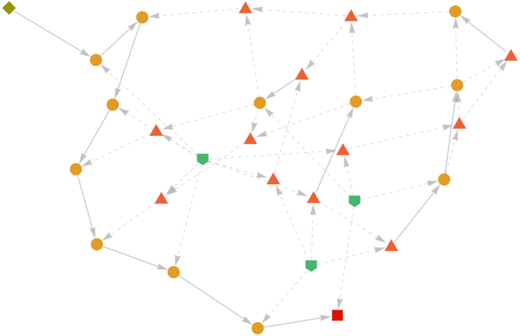

Figure: The proof graph corresponding to the proof of a simple proposition in group theory.

Future Work: HoTT II

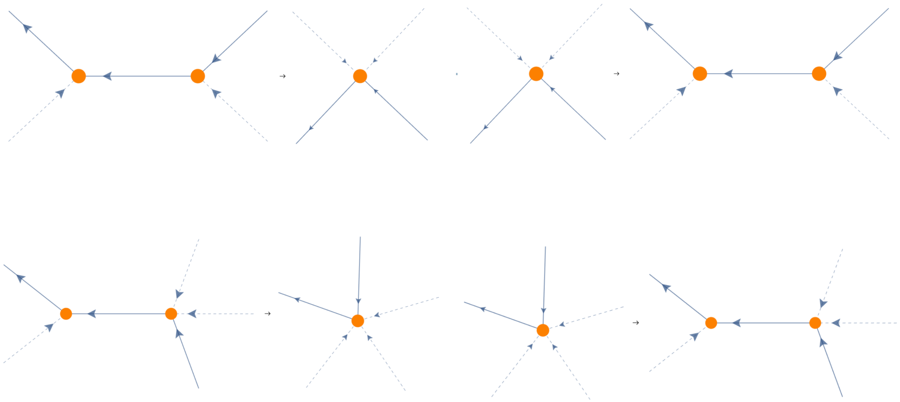

Figure: Diagrammatic inference rules for the fusion/fission operation on substitution lemmas.

Future Work: HoTT III

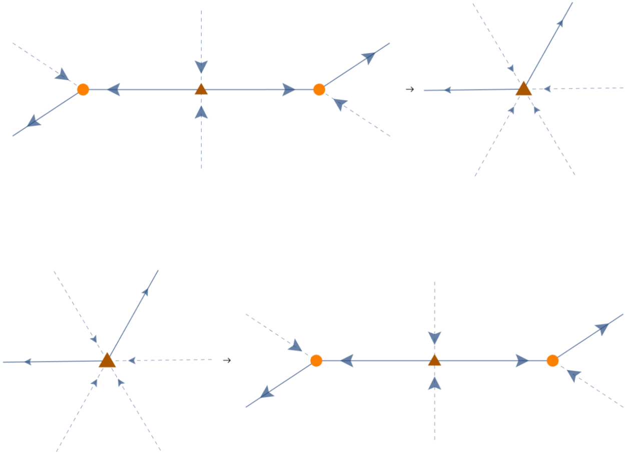

Figure: Diagrammatic inference rules for the compatibility operation between substitution lemmas and critical pair lemmas.

Future Work: HoTT IV

A diagramatic reasoning language for mathematical proofs (and hence homotopy type theory): each multiway system represents the homotopy type for a given logical proposition.

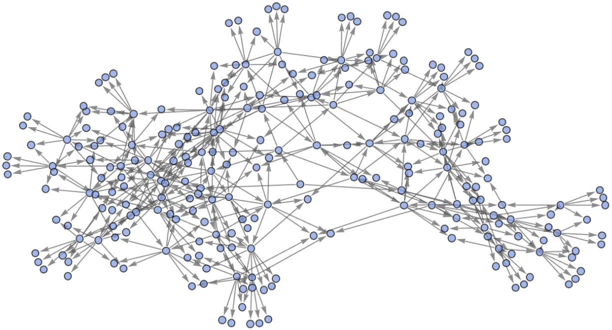

Figure: Multiway states graph corresponding to the first 3 steps in the non-deterministic evolution history of a proof graph multiway system.

Code etc.

All code necessary to reproduce the simulations and visualizations presented here is freely available on the open source *Wolfram Function Repository*, e.g:

- `https://resources.wolframcloud.com/FunctionRepository/resources/MultiwayOperatorSystem`
- `https://resources.wolframcloud.com/FunctionRepository/resources/MakeZXDiagram`
- `https://resources.wolframcloud.com/FunctionRepository/resources/FindWolframModelProof`
- `https://resources.wolframcloud.com/FunctionRepository/resources/QuantumDiscreteStateToZXDiagram`
- `https://resources.wolframcloud.com/FunctionRepository/resources/ZXDiagramToQuantumDiscreteState`
- etc.